Determination of GPS Orbits to Submeter Accuracy

W. I. Bertiger and S. M. Lichten
Tracking Systems and Applications Section

E. C. Katsigris
Geology and Planetology Section

Orbits for satellites of the Global Positioning System (GPS) have been determined with submeter accuracy. Tests used to assess orbit accuracy include orbit comparisons from independent data sets, orbit prediction, ground baseline determination, and formal errors. One satellite tracked for 8 hours each day shows rms errors below 1 m even when predicted more than 3 days outside of a 1-week data arc. Differential tracking of the GPS satellites in high Earth orbit provides a powerful relative positioning capability, even when a relatively small continental U. S. fiducial tracking network is used with less than one-third of the full GPS constellation. To demonstrate this capability, baselines of up to 2000 km in North America were also determined with the GPS orbits. The 2000-km baselines show rms daily repeatability of 0.3 to 2 parts in 10^8 and agree with very-long-baseline interferometry (VLBI) solutions at the level of 1.5 parts in 10^8. This GPS demonstration provides an opportunity to test different techniques for high-accuracy orbit determination for high Earth orbiters. The best GPS orbit strategies included data arcs of at least 1 week, process noise models for tropospheric fluctuations, estimation of GPS solar pressure coefficients, and combined processing of GPS carrier phase and pseudorange data. For data arcs of 2 weeks, constrained process noise models for GPS dynamic parameters significantly improved the solutions.

I. Introduction

The Global Positioning System (GPS), expected to be fully operational by the early 1990s, will consist of 24 satellites evenly spaced in six orbit planes at an altitude of about 20,000 km. Knowledge of GPS orbits will provide the basis for highly accurate ground and satellite user positioning. A wide variety of users will benefit from this positioning capability. GPS will be used at NASA's Deep Space Network (DSN) stations in conjunction with very-long-baseline interferometry (VLBI) radiotelescopes for atmospheric calibrations, precise

ground station position determination, monitoring of Earth orientation changes on time scales of less than one day [1], and possibly time synchronization at the nanosecond level. Differential GPS-based accuracies for high Earth orbiters are expected at the several-meter level for altitudes of 5,000 to 40,000 km [2]. Spacecraft maneuvering near and docking with the Space Station will carry GPS receivers and will use GPS signals for real-time and near-real-time navigation and guidance. Low Earth orbiting spacecraft such as TOPEX/Poseidon [3] and the Earth Observing System platforms will have orbit determination available in post-real time to an

accuracy of better than 10 cm with kinematic smoothing techniques using advanced receivers to track GPS satellites simultaneously with a worldwide GPS ground tracking network. The relatively low cost and convenience of GPS ground receivers have created many new opportunities to monitor cm-level crustal motions in geologically active regions. Very dense ground networks may achieve accuracies equaling or surpassing those available from other generally more restrictive techniques such as VLBI or satellite laser ranging.

The GPS applications with the most stringent requirements include the DSN applications, subdecimeter low Earth orbit determination, cm-level measurements of Earth crustal motion, and cm-level monitoring of changes in Earth orientation. To reach these goals, GPS orbits will have to be determined to better than 50-cm accuracy. The Jet Propulsion Laboratory has been developing and testing GPS orbit estimation software and techniques for several years with the goal of demonstrating the capability for high-accuracy orbit determination. GPS data from several field experiments in 1985 and 1986 have been used to determine precise GPS orbits. Although only seven developmental GPS satellites were operational and the ground fiducial tracking network was limited to sites in the continental United States, covariance studies indicated that with currently available GPS receivers and antennas it should be possible to produce orbits for well-tracked GPS satellites accurate to 1 m. Achieving this 1-m accuracy capability is a major milestone on the road to ultrahigh-precision GPS applications.

In this article we present results demonstrating submeter accuracy for the GPS orbits determined from these field tests. Ground station coordinates were estimated simultaneously along with the orbit parameters. Accuracy of better than 3 cm has been achieved over baselines up to 2000 km, proving that GPS is already a very powerful technique for precise positioning over continental distances.

II. Data Acquisition and Processing

A series of GPS field experiments took place in March and November 1985, June 1986, and January 1988. These experiments were organized by JPL and were cooperative ventures with several different organizations participating. In the March 1985 experiment, data were collected for about 1 week at ground sites in the continental United States only. In November 1985, the tracking network also included three sites in Mexico, and the experiment lasted for about 2 weeks. The June 1986 experiment covered a 3-week period and included sites in the Caribbean region as well as a dense network of stations in Southern California. The data from the experiments up through 1986 has been processed, with the January 1988 data expected to be distributed shortly. This article reports analysis based on the data collected during the November 1985 and June 1986 experiments. Results from the March 1985 experiment have been reported earlier [4], [5].

A. The November 1985 and June 1986 Data Sets

The November 1985 GPS experiment took place from November 12 through November 24. The June 1986 experiment spanned about 3 weeks; the results presented in this article are based on the first part of the experiment from June 2 to June 10. Figure 1 shows the locations of the ground tracking sites, which represent a subset of the total number that participated in the experiments. TI 4100 GPS receivers [6] were operated at most of the sites. SERIES-X(7) receivers[1] built at JPL were used at Mojave and at Owens Valley Radio Observatory (OVRO). In November 1985, water vapor radiometers (WVRs) were available for wet tropospheric delay calibrations at OVRO, at the Mexican sites, and at Mojave for part of the experiment. In June 1986, WVRs were used at Haystack, Mojave, and some of the Caribbean sites. Dry tropospheric delay calibrations were computed from surface measurements of barometric pressure. For receivers located at sites where WVRs were not available, wet tropospheric delay corrections were computed from surface meteorology data. Single-day-arc baseline and GPS orbit solutions were generated for examination of residuals and to check the quality of the data. November 12 and 17 were excluded because of data outages and other difficulties at some of the fiducial sites. For multiday-arc solutions, the November 1985 data set, covering 12 days, was divided first into two arcs of 7 and 5 days (November 13–19 and November 20–24). This was necessary due to a maneuver of more than 100 km which took place on November 20 during which Navstar 4 was moved to a new orbit. Eventually, we modeled and solved for the maneuver as described below, and a single long data arc covering November 13–24 was constructed. During these GPS experiments, periods of common ground visibility lasted about 6 to 8 hours. Most satellites were visible continuously from a given ground station for only about 3 hours, so several times during the tracking period the receivers switched to a new combination. Navstar 8 was unusual in that it was visible for up to 8 hours from most of the ground sites.

Because of the short tracking periods (relative to the GPS orbital period of 12 hours) from a limited network of ground sites, orbits determined from single-day passes in the 1985 and 1986 field tests were significantly weaker than those determined from multiday arcs. The additional strength from the multiday arcs derives mainly from the visibility of the satel-

---

lites from the ground during multiple orbit revolutions. With observations over more than one revolution, the orbital periods are more accurately determined and therefore the positions of the orbital nodes are more precise. The down-track satellite components benefit especially from the multiday arcs, as is sometimes manifested by a corresponding improvement in the eastern component baseline accuracy [5]. A second advantage of multiday-arc solutions is the $\sqrt{n}$ improvement in precision, where n is the number of measurements, which can apply to any orbital or baseline component. As more satellites are launched and the tracking network expands geographically, shorter arcs will achieve the same level of orbit accuracy.

B. Data Collection and Processing

Both GPS carrier phase and pseudorange data were received at all the sites equipped with TI receivers. Carrier phase only was used from the Series-X receivers, which are codeless. The carrier signals at L1 and L2 bands (1.227 and 1.575 GHz) are modulated by a pseudorandom noise code called the P code, which operates at 10.23 MHz. Continuously tracked GPS carrier phase provides a very precise measure of *range change*, while the P code provides a measure of *absolute range*. The pseudorange is considerably noisier than the carrier phase data type, and in this experiment the pseudorange was corrupted by errors due to multipath signals. The GPS observables at the two L-band frequencies are linearly combined to remove the portion of ionospheric delay which varies as the inverse square of the frequency. For more details about the characteristics of the GPS signals, see [7] and [8]. Hereafter, the terms "carrier phase" and "pseudorange" refer to these linear combinations of L1, L2 and P1, P2. The GPS data were processed with the GPS Inferred Positioning SYstem (GIPSY) orbit determination and baseline estimation software, which was completed and tested at JPL shortly after the data were collected for the 1985 experiments.

III. Orbit Determination Approach

The JPL orbit determination software utilizes a pseudoepoch-state U-D factorized Kalman filter[2] [9]. The filter works as a batch sequential program with the option to model parameters as first-order exponentially correlated process noise, also commonly called colored noise. The GIPSY software uses the J2000 reference system with observation partials for parameters computed relative to the satellite epoch states [10].

For the November 1985 data set, the nominal GPS ephemerides were obtained by using broadcast orbits as initial values

and iterating to improve those orbits (and remove large undesired offsets resulting from different coordinate frame conventions) with a small subset of the data. During the iteration, GPS solar radiation pressure coefficients were also determined and these coefficients and the new orbits were used as nominal values for the more comprehensive precise orbit filter runs. In June 1986, the hybrid postfit ephemeris from the Naval Surface Weapons Center (NSWC) was used for nominal trajectories and a similar iteration was performed prior to the final filter solutions.

The high-precision orbit determination strategy used with the November 1985 and June 1986 GPS data was based on previous experience with the March 1985 GPS experiment [5]. A key aspect of the orbit estimation process is the fiducial concept, where three or four receivers with well-known coordinates in a consistent reference frame are held fixed while all other parameters, including orbital states and coordinates of the nonfiducial sites, are estimated simultaneously in the filter. Reference 5 and the references therein discuss the fiducial concept as well as alternative approaches. The fiducial receivers for the experiments discussed in this article were collocated at VLBI sites. Haystack, Richmond, and Fort Davis were generally treated as fiducials. In some runs OVRO was held fixed, and in others Hat Creek was used as a fiducial so that one of the normally fixed receivers could be estimated using the GPS data in order to test the internal consistency. As more GPS satellites are launched and the ground tracking network is expanded from North America to include stations on other continents, we expect that fewer fiducial constraints will need to be applied and more station location parameters will be determined from the GPS data.

A. Clock and Bias Parameters

The results presented here are based on estimation of station and GPS clocks as white process noise. At each measurement epoch, each active clock is assumed to have a value uncorrelated to its value at other epochs. Although some station clocks were running off hydrogen masers and most of the GPS clocks have well-characterized behavior typical of rubidium and cesium atomic standards, this extra information was not used. The white noise clocks were estimated simultaneously with the other parameters in the filter. When the process noise model for clocks is white noise, the results are virtually the same as would be achieved with double differencing [11] for clock elimination.

The GPS carrier phase, when continuously tracked, provides a very precise measure of range change from measurement epoch to measurement epoch. The absolute phase, however, and hence the absolute range from transmitter to receiver, is ambiguous by an integral number of wavelengths. For each station-satellite tracking pass, a carrier phase bias parameter is

---

[2]S. C. Wu, W. I. Bertiger, J. S. Border, S. M. Lichten, R. F. Sunseri, B. G. Williams, P. J. Wolff, and J. T. Wu, "OASIS Mathematical Description, v. 1.0," JPL Internal Document D-3139, Jet Propulsion Laboratory, Pasadena, California, 1986.

estimated, along with the other adjusted parameters, ignoring the integer constraint on its value. Over a period of hours, the signature of the *range change* precisely measured with the carrier phase enables the orbit to be determined. The pseudorange, on the other hand, provides a more direct range determination but is much noisier and more susceptible to multipath errors than the carrier phase data type. The ultimate accuracy would be reached if *carrier range* were available. Carrier range is a range determined from carrier phase with the bias ambiguities all resolved; it has the best features of both carrier phase (low noise, low multipath) and pseudorange (absolute range measure and geometric strength). Successful carrier phase ambiguity resolution has been reported over baselines of up to 2000 km with *bias fixing* or *bias optimizing* techniques applied to single-day arcs [12], [13]. The results reported here were achieved by estimation of the white noise clock and carrier phase bias parameters with a very large a priori uncertainty, so that their solutions were basically unconstrained. Bias fixing was not used to resolve the carrier phase ambiguities.

B. Tropospheric Delay Fluctuations

The troposphere was modeled as a spherical shell which adds a delay along the GPS signal path:

$$\rho = \rho_{z_d} R_d(\theta) + \rho_{z_w} R_w(\theta) \qquad (1)$$

where ρ_z is the zenith tropospheric path delay and R is an analytic mapping function [14] to map zenith delays to line-of-sight path delays at elevation θ. There are two components to the tropospheric delay—the wet and the dry, denoted here with subscripts w and d. The dry component can be determined under the assumption of hydrostatic equilibrium using the ideal gas law for dry air to better than 1 cm [15]. The wet delay component, although considerably smaller than the dry, exhibits greater time and spatial variation and is much more difficult to determine accurately.

WVRs were operated at some of the GPS tracking sites alongside the GPS receivers. WVR calibrations are believed accurate to 2 cm or better for determination of the wet zenith path delay [15]. The algorithm described in [16] was used to determine these calibrations. At the other sites, surface meteorology (SM) measurements (temperature, air pressure, and relative humidity) were used for the wet zenith delay calibration [17]. The SM calibration is much less reliable than the WVR calibration because the surface meteorological conditions are not always well correlated with the total atmospheric water vapor content [15].

Wet zenith delay corrections to the calibrations (WVR or SM) were estimated with the GPS data for all GPS tracking sites. For most sites with WVRs, a constant wet zenith delay

parameter with an a priori constraint of 3 cm was estimated for each 8-hour tracking day. For sites using SM calibrations, the wet zenith delay was estimated daily with a 20-cm a priori constraint. In addition, stochastic residual delays were estimated for SM sites in order to remove signatures which could result from temporal variations in the troposphere, time-varying errors in the SM calibrations, errors in the mapping function, or spatial inhomogeneities due to azimuthal asymmetry in the water vapor content. In some cases, tightly constrained process noise troposphere residual delay parameters were also estimated for the WVR sites.

C. Troposphere Process Noise Models

The stochastic model in the GIPSY filter is for a first-order exponentially correlated process noise [9]. The measurements are processed in discrete time segments, known as *batches*. In each batch, process noise parameters are modeled as piecewise constants. At the end of a batch, a process noise time update adds noise to the covariance matrix and thus causes the time-varying behavior of the stochastic parameters. The process noise time update for the jth batch maps the estimates and covariance for the stochastic parameters into batch $j + 1$:

$$\mathbf{p}_{j+1} = \mathbf{M}_j \mathbf{p}_j + \mathbf{w}_j \qquad (2)$$

where $\mathbf{p}_j$ is a vector of estimates for the stochastic parameters and $\mathbf{M}$ is a diagonal process noise mapping matrix. The process noise $\mathbf{w}_j$ is a random process with zero mean and

$$E\left(\mathbf{w}_j \mathbf{w}_k^T\right) = \mathbf{Q}\delta_{jk} \qquad (3)$$

where $\mathbf{Q}$ is the covariance matrix diagonal and δ_{jk} is the Kronecker delta function [9]. The diagonal entries of $\mathbf{M}$ are given by

$$m_{ij} = \exp\left[-(t_{j+1} - t_j)/\tau_{ij}\right] \qquad (4)$$

where t_j is the start time for the jth batch and τ_{ij} is the time constant for the ith stochastic parameter at the jth batch. The corresponding diagonal entry in the matrix $\mathbf{Q}$ is

$$q_{ij} = \left(1 - m_{ij}^2\right)\sigma_{iss}^2 \qquad (5)$$

where σ_{iss}, the steady-state sigma for the ith stochastic parameter, is the noise level that would be reached if the system were left undisturbed for a time much greater than τ. The process noise model for each parameter is fully specified by σ_{ss} and τ, which can also vary with time, although the subscript j has been left off σ_{ss} for simplicity of notation. There are two special limiting cases: white process noise, and a ran-

dom walk. For white process noise, $\tau = 0$, $m = 0$, and, as can be seen in Eq. (2), the a priori covariance for the process noise parameters, p, is completely reset at the end of each batch, including zeroing of off-diagonal terms and inserting q for the variance on the diagonal. For white noise, the process at each time step is independent and uncorrelated with the process at other time steps. The opposite case is the random walk. Here both σ_{ss} and τ are unbounded, since a steady state is never reached and $\tau = \infty$. For the random walk, however, q is still defined by Eq. (2), where M is now equal to the identity matrix. The Allan variance [18], $\sigma_A^2 (\Delta t)$, which is often used to characterize clock and atmospheric fluctuations [19], is directly related to the random walk q:

$$\sigma_A^2 (\Delta t) = q/\Delta t^2 \quad \text{(random walk)} \quad (6)$$

A wide range of process noise models has been tested on the March and November 1985 and June 1986 GPS data sets [5], [15], [20]. The random walk zenith tropospheric delay models with $\sqrt{q}$ in the range 2 to 4×10^{-7} km·s$^{-1/2}$ (for SM sites) produced the best daily baseline repeatability, agreement with VLBI, and orbit repeatability. When only constant zenith delay parameters were estimated, orbit and baseline accuracies were worse by about a factor of 2. The value of $\sqrt{q}$ adopted for most of the November 1985 and June 1986 analyses was 2×10^{-7} km·s$^{-1/2}$, corresponding to about 6 cm variation over a 24-hr period. There is evidence from VLBI residuals [19], [21] that tropospheric delay and delay-rate fluctuations can be well modeled as random walks for Δt greater than a few hundred seconds. Since the GPS data were compressed to 300-sec intervals, the use of random walk tropospheric fluctuation models for GPS is consistent with the VLBI findings. As discussed in [5], however, the GPS process noise parameters were used to estimate a fluctuating *residual* correction to calibrated data (WVR or SM), and it is not clear that this quantity will have the same stochastic characteristics as the tropospheric fluctuations themselves. It was assumed that the spectral characteristics of both the tropospheric fluctuations and the residuals after calibration would be similar.

D. Solar Radiation Pressure and Other Nongravitational Forces

Multiday arcs covering 1 to 2 weeks were used to achieve the highest GPS orbit accuracy. With a global tracking system equipped with high-performance GPS receivers and a full 24-satellite GPS constellation, covariance analysis predicts GPS orbit accuracy well below 1 m after just several hours of tracking [22]. However, as can be seen from Fig. 1, the ground tracking network during 1985 and 1986 was limited, with fiducials in North America only. The seven GPS satellites that were operating at that time by design tend to converge

over the southwest United States. This further limited common ground visibility to less than 8 hours per day and reduced the geometrical strength of the system. In addition, the pseudorange available from the TI receivers that were used in 1985 and 1986 was highly contaminated by ground multipath, thereby raising the effective measurement noise. Because of these factors, multiday arcs were necessary to achieve the desired improvement in ephemeris accuracy.

With single-day (8-hour) orbit solutions, there is very little sensitivity to errors in the GPS solar radiation pressure coefficients [4]. However, for multiday arcs with multiple orbit revolutions, the orbital period is much more accurately determined and therefore the results become sensitive to downtrack errors resulting from integration of accelerations due to solar radiation forces acting on the GPS satellites, mismodeled solar radiation, or unmodeled forces such as thermal radiation from the spacecraft body. The GPS Block I ROCK4 model was used to represent accelerations resulting from solar radiation pressure. As described in [5] and references therein, ROCK4 models 13 surfaces on the satellites according to their size, curvature, reflectivity, specularity, and absorption characteristics. The model as implemented in GIPSY allows for adjustment of three parameters: G_x, G_y, and G_z. G_x and G_z are scaling factors in the local spacecraft x and z directions, where the z axis is positive along the antenna toward the center of the Earth, the y axis is along the solar panel support beam normal to the spacecraft-Sun-Earth plane, and the x axis completes a right-handed coordinate system. G_y represents a constant acceleration in the y-axis direction, often referred to as the y-bias parameter [23].

In principle, the G_x and G_z parameters should have the same value if the spacecraft were perfectly aligned and the model were correct. GPS orbits have been determined in the past with estimation of only G_y and one parameter (designated here as G_{xz}) to represent both G_x and G_z [24], [25]. For the multiday arcs determined with the March 1985 data [5], G_x, G_y, and G_z were estimated independently as constants for each satellite with the intention of adding an extra degree of freedom ($G_x \neq G_z$) to absorb unmodeled accelerations and known deficiencies in the ROCK4 model, which are thought to amount to as much as 4 m error over a 14-day prediction interval [23]. This strategy was successful for data arcs up to about 1 week long. However, for longer arcs of up to 2 weeks, a noticeable and systematic degradation in daily baseline repeatability occurred with the three-parameter constant solar coefficient approach. A new approach was adopted in which two constant solar pressure coefficients were estimated, G_y and G_{xz}, along with two tightly constrained process noise parameters, G_x and G_z. With this approach, daily baseline repeatability continued to improve as the arc was lengthened.

As an alternative to the use of process noise on G_x and G_z, small colored noise accelerations were introduced for the long November 13–24 arcs. These consisted of three parameters representing a constant thrust in the directions of down-track, cross-track, and altitude.

Both stochastic solar pressure parameters and stochastic thrust parameters gave similar repeatability results for the 2-week data arc, Fig. 2. The results were insensitive to the time constant, τ, as long as the value of q was held about constant (see Eqs. 4 and 5). For G_x and G_z, τ was varied from 1 to 28 days with $q \approx 9.3 \times 10^{-6}$, and the repeatability results were essentially the same. The results for the thrust parameters were more sensitive to the time constant. The best results were not obtained until the time constant was made less than 2 days and the value of $q \approx 2 \times 10^{-28}$ km^2/sec^4. Similar results were obtained when the time constant for the thrust parameters was made as short as 0.5 day. A single stochastic thrust in the direction of the satellite long track also yielded good repeatability. With the present data, which consists of relatively short arcs at the same time each day, one cannot determine whether the effects are due to solar pressure mismodeling or other random or systematic accelerations acting on the GPS spacecraft. One possibility is that a solar pressure stochastic model is physically the correct approach but the stochastic fictitious thrust model works as well, as long as the thrust time constant is short enough to absorb the daily variations implicit in the solar radiation pressure signature. Note that another approach to this problem has been proposed in which fictitious force parameters with 24-hr resonances are estimated to remove solar pressure, gravity, and other dynamic errors which tend to repeat daily [28]. It is hoped that the sources of these forces can be isolated when more data and global tracking are available. This may be possible with the CASA UNO data set [29].

E. GPS 4 Maneuver

A maneuver was performed on GPS 4 (SV 8) at approximately UT 0320 November 20, 1985. In a few hours the spacecraft state was changed by over 100 km and it was moved to a slightly different orbit. This time was in the middle of the experiment but outside the data collection interval, which was from about UT 1100–1900 each day. In order to perform continuous orbit determination over the entire experiment interval (November 13–24) for all the satellites simultaneously, we had to model and estimate the maneuver. The NSWC parameterized the maneuver as a constant thrust over 5 minutes. We used a four-parameter model with three instantaneous velocity changes and a time-of-burn parameter, which we refer to as an impulsive motor burn. The impulsive motor burn allows for an instantaneous change in position and velocity while leaving the acceleration unchanged. Let ΔV be the vector velocity increment, with three components ΔV_H, ΔV_C, and ΔV_L, where

subscripts H, C, and L refer to the local spacecraft coordinates of altitude, cross-track, and down-track. Let ΔT_B denote the time of burn, e.g., the interval over which the burn is applied. Then the vector change in position is

$$\Delta r = \frac{1}{2} \Delta V T_B = \frac{1}{2} a \Delta T_B^2 \qquad (8)$$

The acceleration, a, defined by ΔV and ΔT_B, is the equivalent constant acceleration that would be experienced over the interval ΔT_B. The solution for the maneuver parameters ΔV_H, ΔV_C, ΔV_L, and ΔT_B was obtained by iterating over a data arc spanning November 18–22. The maneuver solution converged after three iterations and showed meter-level agreement with a separate solution for the GPS 4 position using only data collected after the maneuver (November 20–24). This nominal representation for the maneuver was further refined in later longer-arc high-precision GPS orbit solutions. It is interesting to note that the maneuver solution did not converge initially unless we constrained $G_x = G_z$ for GPS 4.

IV. Assessment of Orbit Accuracy

Five criteria were used to assess the accuracy of the GPS orbits determined from multiday arcs in November 1985 and June 1986: (1) orbit repeatability; (2) orbit prediction; (3) daily baseline repeatability; (4) agreement between GPS and VLBI-determined baselines; and (5) formal errors from the orbit filter.

A. Orbit Repeatability

Orbit repeatability indicates the precision and, to some extent, the accuracy of the GPS orbits. Figure 3 illustrates how orbit repeatability was computed for the November 1985 experiment. The purpose of orbit repeatability is to compare orbits determined independently without any common measurements and then compute the rms difference over a time interval during which no data were used for either of the two solutions. Figure 4 shows the mean of the rms computed for all seven GPS satellites over a 6-hr interval on November 17. Figure 4 also shows the significant improvement attained when pseudorange is processed with the carrier phase and stochastic tropospheric delay models are used. From the formal errors, it appears that the pseudorange contributed little geometric strength to the orbit solutions, since the rms scatter of individual measurements was 100 to 300 cm for 6-minute measurement intervals, due mostly to ground multipath. However, when the pseudorange and carrier phase are processed together and a common clock is estimated, the pseudorange provides a priori knowledge of the clock and carrier phase bias parameters at the several-nanosecond (100–300 cm) level, significantly improving the orbits.

GPS 6 and 8, the two satellites with the most data and best ground viewing geometry, had formal errors below 1 m for most of the November experiment and had significantly lower orbit repeatability rms than the other satellites. Figure 5 shows the repeatability computed over a 24-hr interval on November 17 when no measurements were used for either orbit solution. Since the two solutions being compared were determined from independent data sets (Fig. 3), it is concluded that sub-meter orbit precision has been demonstrated for these two satellites.

B. Orbit Prediction

Orbit prediction is a stringent test of orbit accuracy, since the estimated spacecraft position and velocity are mapped outside of the measurement interval to give a predicted satellite state. Orbit errors tend to be magnified in this mapping process. The accuracy of the orbit models used for mapping are also tested by the orbit prediction test, in addition to the accuracy of the satellite ephemerides. Figure 6 shows the prediction test we applied to our November 1985 multiday-arc orbits. The average rms errors for four of the satellites were 0.7 m, 0.8 m, and 1.7 m in altitude, cross-track, and down-track components. GPS 8, which was tracked longer than any of the other satellites, had a prediction rms error well below 1 m, even when mapped more than 3 days into the second arc. For the first 6 hours of the prediction interval, the rms error was 50 cm or less for all three position components. These results are shown in Figs. 7 and 8.

C. Daily Baseline Repeatability and Agreement Between GPS and VLBI Solutions

To further assess the GPS orbit accuracy determined with multiday arcs, we have examined daily baseline repeatability as well as agreement with independent VLBI baseline measurements over continental distances (1000 to 2000 km). For the November 1985 experiment, we examined baselines between Hat Creek, CA and Fort Davis, TX (1933 km); Mojave, CA and Fort Davis, TX (1314 km); and Richmond, FL and Haystack, MA (2046 km). Daily repeatability was computed as the rms about the weighted mean of the daily baseline solutions determined simultaneously with one multiday-arc orbit solution. For these baselines in North America with good common visibility of the GPS, the rms scatter was 0.3 to 2 parts in 10^8 of baseline length for all vector components. Agreement with VLBI was 0.3 to 1.5 parts in 10^8 for baselines with the same type of GPS antenna at both ends. Figures 9 and 10 show the results for the 2000-km baselines.

For determination of the Hat Creek–Fort Davis baseline, Fort Davis, Richmond, and Haystack were held fixed as fiducial stations. For the Richmond–Haystack baseline solution, a separate filter run was made with Hat Creek, Fort Davis, and

Haystack fixed as the fiducial reference points. Note that in the case of the Richmond–Haystack baseline the Hat Creek fiducial does not have data in the second half of the 2-week data arc, reducing the number of fiducials to two for the second half. The data from the first half has already determined the GPS positions sufficiently that the lack of a third fiducial does not degrade the quality of the solution. Although high-quality orbits are a prerequisite for good precision and accuracy over long baseline distances, there are other factors that can affect baseline accuracy aside from GPS orbits. For example, local site vectors between the GPS and VLBI antennas sometimes are inaccurate by several cm. One such local survey error was recently discovered at OVRO, leading to a 5-cm discrepancy between the GPS and VLBI Mojave–OVRO baseline until it was corrected [26]. Therefore, while the daily baseline repeatability provides a measure of consistency for orbits determined from multiday arcs, agreement with VLBI is a measure of *overall system accuracy*, which depends on a number of factors in addition to orbit accuracy.

When different GPS antennas were used at the ends of a baseline, although daily repeatability was excellent, agreement with VLBI was worse by 1 to 7 cm, with no apparent dependence on baseline length. This was noticed in both the November 1985 and June 1986 experiments. However, baselines with the same type of GPS antennas showed good agreement with VLBI. Since ephemeris errors tend to scale with baseline length, it was hypothesized that these discrepancies were due to local phenomena rather than orbital effects. Attention has been directed at phase center variations in the antennas, since the TI antennas are designed so that in operation the phase center variations nearly cancel out between sites that are not more than a few thousand km apart [6]. However, the Series-X antennas do not have the same phase center characteristics as the TI antennas, and the signatures resulting from the several-cm phase center variations that have been measured [27] could corrupt baseline measurements between unlike antennas. Therefore we qualify our high-precision results with the warning that measurements between different GPS antennas may be much less reliable and may be affected by unpredictable effects.

D. Baseline Repeatability Outside the Fiducial Network

The baselines in North America are fairly well determined because they are either inside or near the fiducial network and because the current limited GPS constellation by design is optimized for North America, especially the southwest United States. The formal errors from the filter are consistent with the results in Figs. 7, 8, and 9, predicting precision of 1 to 4 cm over these 2000-km baselines. To further test the robustness of the multiday-arc GPS orbits, we have determined baselines between Richmond and several sites in the Caribbean Sea

region occupied during the June 1986 experiment. Figure 10 shows daily baseline repeatability for Richmond–Grand Turk (1049 km) and Richmond–Isabela (1582 km) determined from an 8-day orbit fit for June 2–10, 1986. Because the Caribbean sites are far to the southeast of both the fiducial network and the optimal region for the GPS constellation, the formal errors for these baselines are typically 2 to 7 cm, somewhat worse than those of the North American baselines. Despite the degraded geometry and reduced common visibility, the baselines to the Caribbean sites show precision of 1 to 4 parts in 10^8. Some of the Caribbean sites were equipped with WVRs; for these as well as the sites without WVRs, residual tropospheric corrections determined from the GPS data were critical in achieving these levels of baseline precision. Since the Caribbean sites are considerably more humid than most of the North American sites, various strategies for reducing systematic errors due to uncertainties in the wet troposphere correction are being studied with this data set.

V. Conclusions

It has been demonstrated that submeter GPS orbits can be determined using multiday arc solutions with the current GPS constellation subset visible for about 8 hours each day from North America. Submeter orbit accuracy was shown through orbit repeatability and orbit prediction. North American baselines of 1000 to 2000 km in length can be estimated simultaneously with the GPS orbits to an accuracy of better than 1.5 parts in 10^8 (3 cm over a 2000-cm distance) with a daily precision of 2 parts in 10^8 or better. The most reliable baseline solutions are obtained using the same type of receivers and antennas at each end of the baseline. Baselines longer than

1000 km between Florida and sites in the Caribbean region have also been determined with daily precision of 1 to 4 parts in 10^8. The Caribbean sites are located well outside the fiducial tracking network and the region of optimal GPS common visibility, so these results further demonstrate the robustness of the multiday-arc GPS orbit solutions.

Process noise models have been used in the orbit determination filter to minimize systematic errors which can seriously affect ephemeris and baseline accuracy. These systematic effects include tropospheric delay fluctuations and small, unmodeled spacecraft accelerations. The process noise troposphere models improved all orbit and baseline solutions, regardless of length of data arc. Tightly constrained process noise representation for part of the solar pressure model significantly improved baseline repeatability for arcs longer than 1 week; however, an equally effective technique had fictitious thrusts estimated stochastically for each GPS satellite. Because of the limited ground visibility with the current constellation, it is not yet possible to determine whether the accelerations are genuinely related to solar radiation pressure or are due to other random or systematic forces acting on the spacecraft.

This demonstration of several-cm accuracy over distances of a few thousand km, despite a limited ground tracking network and a constellation of only seven satellites, proves that GPS provides a very powerful relative positioning capability. It shows that GPS techniques have the intrinsic data strength and robustness needed for DSN high-precision applications, as well as low Earth orbiter tracking and crustal motion studies.

References

[1] A. P. Freedman and J. O. Dickey, "Usefulness of GPS for the Precise Determination of Earth Orientation Parameters," *EOS*, vol. 68, no. 44, p. 1245, November 3, 1987.

[2] S. C. Wu, "Differential GPS Approaches to Orbit Determination of High-Altitude Earth Satellites," AAS/AIAA Astrodynamics Specialist Conference, paper AAS 85-430, August 12–15, 1985, Vail, CO, published in *Astrodynamics 1985*, vol. 58 of *Advances in the Astronautical Sciences*, pp. 1203–1220, 1986.

[3] S. M. Lichten, S. C. Wu, J. T. Wu, and T. P. Yunck, "Precise Positioning Capabilities for TOPEX Using Differential GPS Techniques," AAS/AIAA Astrodynamics Specialist Conference, paper AAS 85-401, August 12–15, 1985, Vail, CO, published in *Astrodynamics 1985*, vol. 58 of *Advances in the Astronautical Sciences*, pp. 597–614, 1986.

[4] J. M. Davidson, et al., *The Spring 1985 High Precision Baseline Test of the JPL GPS-Based Geodetic System*, JPL Publication 87-35, November 15, 1987.

[5] S. M. Lichten and J. S. Border, "Strategies For High Precision GPS Orbit Determination," *J. Geophys. Res.*, vol. 92, pp. 12751–12762, November 10, 1987. November 10, 1987.

[6] D. J. Henson, E. A. Collier, and K. R. Schneider, "Geodetic Applications of the Texas Instruments TI 4100 GPS Navigator," *Proceedings First International Symposium on Precise Positioning with GPS-1985*, vol. I, pp. 191–200, National Geodetic Information Center, NOAA, Rockville, MD, 1985.

[7] R. J. Milliken and C. J. Zoller, "Principle of Operation of NAVSTAR and System Characteristics," *Navigation*, vol. 25, pp. 95–106, 1978.

[8] E. H. Martin, "GPS User Equipment Error Models," *Navigation*, vol. 25, pp. 201–210, 1978.

[9] G. J. Bierman, *Factorization Methods for Discrete Sequential Estimation*, Orlando, Florida: Academic Press, 1977.

[10] O. J. Sovers and J. S. Border, *Observation Model and Parameter Partials for the JPL Geodetic GPS Modeling Software*, GPSOMC, JPL Publication 87-21, September 15, 1987.

[11] Y. Bock, S. A. Gourevitch, C. C. Counselman III, R. W. King, and R. I. Abbot, "Interferometric Analysis of GPS Phase Observations," *Manuscr. Geod.*, vol. 11, pp. 282–288, 1986.

[12] D. Dong and Y. Bock, "GPS Network Analysis: Ambiguity Resolution," *EOS*, vol. 69, no. 16, p. 325, April 19, 1988.

[13] G. Blewitt, "Successful GPS Carrier Phase Resolution for Baselines up to 2000 km in Length," *EOS*, vol. 69, no. 16, p. 325, April 19, 1988.

[14] G. Lanyi, "Troposphere Calibration in Radio Interferometry," *Proceedings of the International Symposium on Space Techniques for Geodynamics*, pp. 184–195, IAG/COSPAR, Sopron, Hungary, July 1984.

[15] D. M. Tralli, T. H. Dixon, and S. A. Stephens, "The Effect of Wet Tropospheric Path Delays on Estimation of Geodetic Baselines in the Gulf of California Using the Global Positioning System," *J. Geophys. Res.*, vol. 93, pp. 6465–6557, June 10, 1988.

[16] S. E. Robinson, "A New Algorithm for Microwave Delay Estimation From Water Vapor Radiometer Data," *TDA Progress Report 42-87*, vol. July–September 1986, pp. 149–157, Jet Propulsion Laboratory, Pasadena, CA, November 15, 1986.

[17] C. C. Chao, "A New Method to Predict Wet Zenith Range Correction from Surface Measurements," *JPL Technical Report 32-1526, vol. XIV, The Deep Space Network*, pp. 33–41, Jet Propulsion Laboratory, Pasadena, CA, 1974.

[18] D. W. Allen, "Statistics of Atomic Frequency Standards," *Proc. IEEE*, vol. 54, pp. 221–230, 1966.

[19] A. R. Thompson, J. M. Moran, G. W. Swenson, *Interferometry and Synthesis in Radio Astronomy*, New York: John Wiley & Sons, 1986.

[20] E. C. Katsigris, D. M. Tralli, and T. H. Dixon, "Estimation of Wet Tropospheric Path Delays in GPS Baseline Solutions for the 1986 Caribbean Experiment," *EOS*, vol. 69, no. 16, p. 324, April 19, 1988.

[21] R. N. Treuhaft and G. E. Lanyi, "The Effect of the Dynamic Wet Troposphere on Radio Interferometric Measurements," *Radio Science*, vol. 22, pp. 251–265, 1987.

[22] W. G. Melbourne, G. Blewitt, S. M. Lichten, R. E. Neilan, S. C. Wu, and B. E. Schutz, "Establishing a Global GPS Tracking System for Fiducial Control and Ephemeris Production," *EOS*, vol. 69, p. 323, no. 16, April 19, 1988.

[23] H. F. Fliegel, W. A. Feess, W. C. Layton, and N. W. Rhodus, "The GPS Radiation Force Model," *Proceedings First International Symposium on Precise Positioning with GPS-1985*, vol. I, pp. 113–120, National Geodetic Information Center, NOAA, Rockville, MD, 1985.

[24] E. R. Swift, "NSWC's GPS Orbit/Clock Determination System," *Proceedings First International Symposium on Precise Positioning with GPS-1985*, vol. I, pp. 51–62, National Geodetic Information Center, NOAA, Rockville, MD, 1985.

[25] R. I. Abbot, Y. Bock, C. C. Counselman III, and R. W. King, "GPS Orbit Determination," *Proceedings Fourth International Geodetic Symposium on Satellite Positioning*, Defense Mapping Agency and National Geodetic Survey, vol. I, pp. 271–273, Austin, TX, April 1986.

[26] J. Ray, "MOTIES Results," presented at the Crustal Dynamics Investigators Meeting, Jet Propulsion Laboratory, Pasadena, CA, March 22, 1988.

[27] A. Kleusberg, "GPS Antenna Phase Centre Variations," *EOS*, vol. 67, no. 44, p. 911, Nov. 4, 1986.

[28] O. L. Colombo, "Precise Determination of GPS Orbits and Station Positions," presented at IUGG Symposium, Vancouver, BC, August 1987.

[29] R. E. Neilan, et al., "CASA UNO GPS–A Summary of the January '88 Campaign," *EOS*, vol. 69, no. 16, p. 323, April 19, 1988.
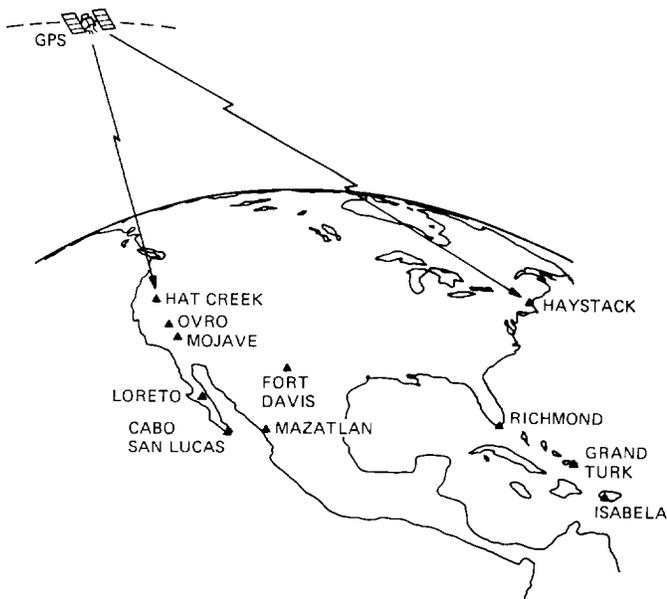
Fig. 1. Locations of ground tracking sites used in the analysis of GPS data from the November 1985 and June 1986 experiments.

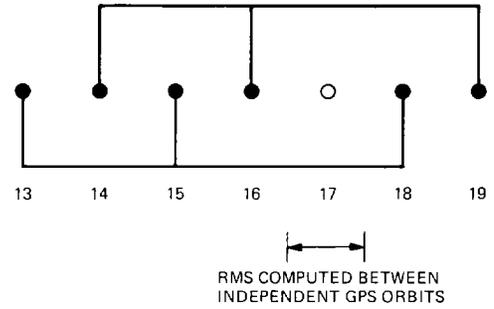RMS COMPUTED BETWEEN
INDEPENDENT GPS ORBITS

Fig. 3. Orbit repeatability for November 1985 uses data from Nov. 13, 15, 18 for one solution and Nov. 14, 16, 19 for the other. Rms difference between the two solutions is computed over Nov. 17, during which no data was taken.
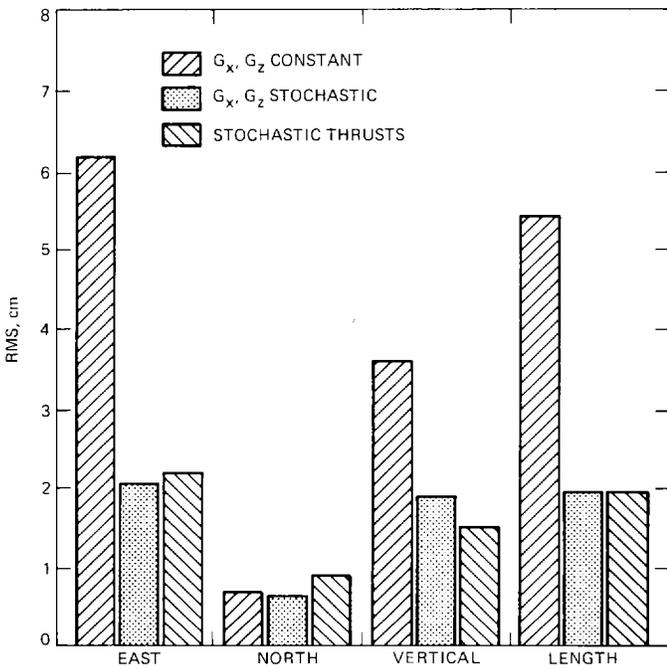

Fig. 2. Daily baseline repeatability with 2-week orbit arcs (Nov. 13-24, 1985) for the Mojave-Fort Davis 1314-km baseline showing dramatic improvement when stochastic force parameters are estimated for GPS satellites.
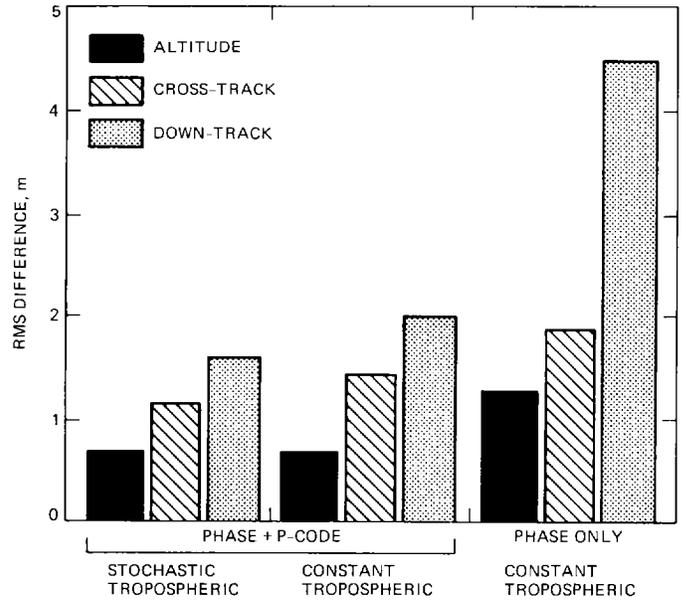
Fig. 4. Rms orbit repeatability over a 6-hr interval on Nov. 17. Rms between independent arcs shown in Fig. 3 for altitude, cross-track, and down-track components have been averaged for all seven GPS satellites.

24
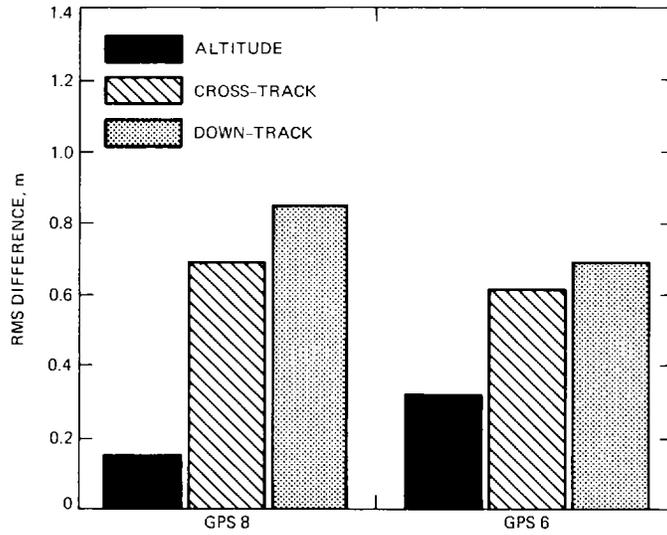
Fig. 5. Submeter orbit repeatability for GPS 6 and 8. Rms difference between two independent solutions is computed over a 24-hr interval on Nov. 17 when no measurements were used.
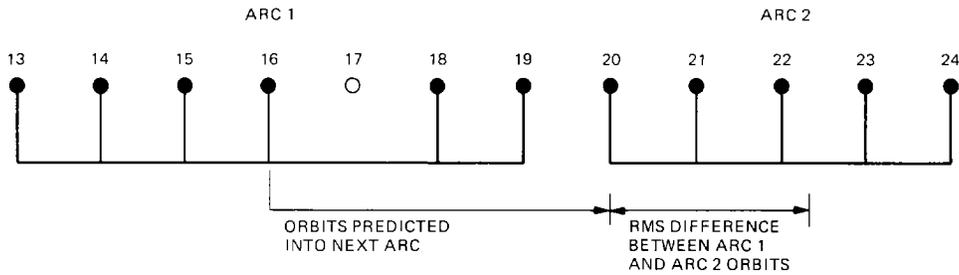

Fig. 6. Orbit prediction test for Nov. 1985. Orbits determined from Nov. 13-19 are mapped ahead, and the rms difference is computed with an independent solution determined from Nov. 20-24.
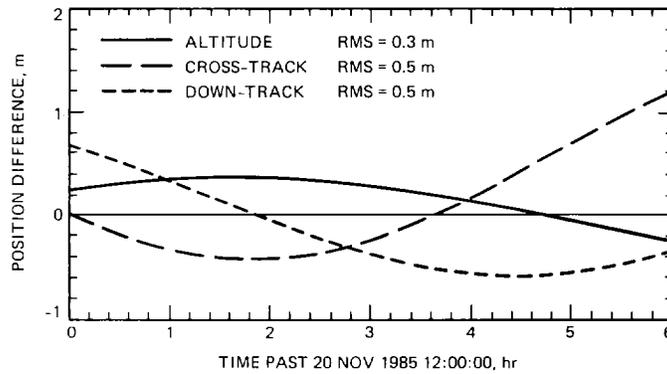

TIME PAST 20 NOV 1985 12:00:00, hr

Fig. 7. Difference between arc 1 predicted orbit and arc 2 orbit as shown in Fig. 6 for GPS 8. Rms is taken over a 6-hr interval.
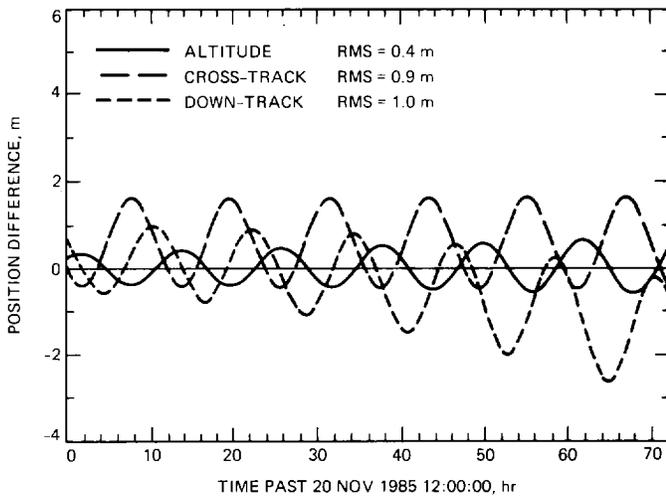
Fig. 8. Orbit prediction difference similar to Fig. 7 except that here the difference and rms are shown for a prediction interval of more than 3 days.
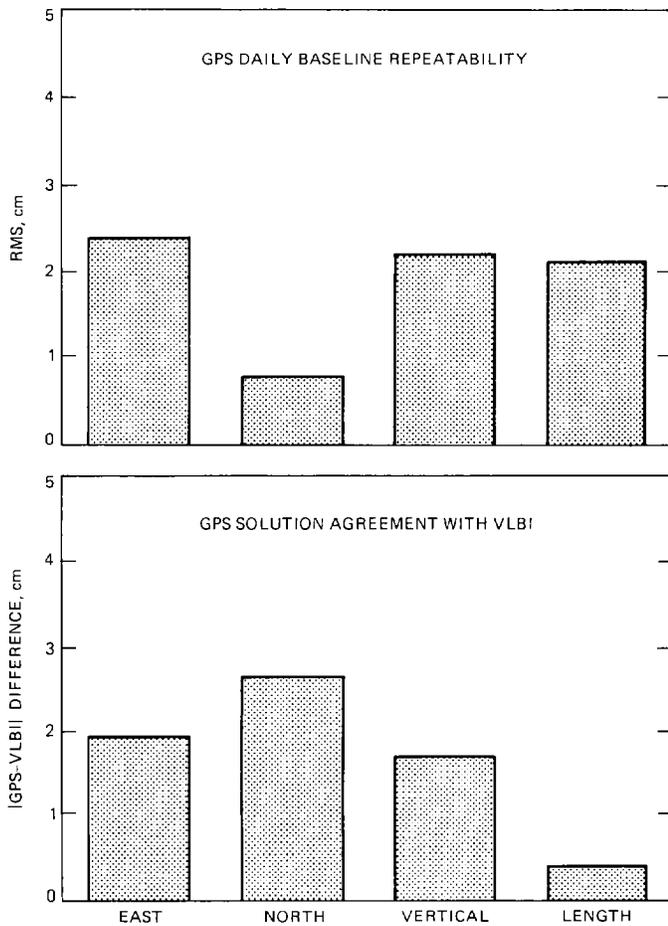

Fig. 9. Daily GPS baseline repeatability and agreement with VLBI for the Hat Creek-Fort Davis 1933-km baseline determined with a multiday orbit fit from Nov. 13-24, 1985.
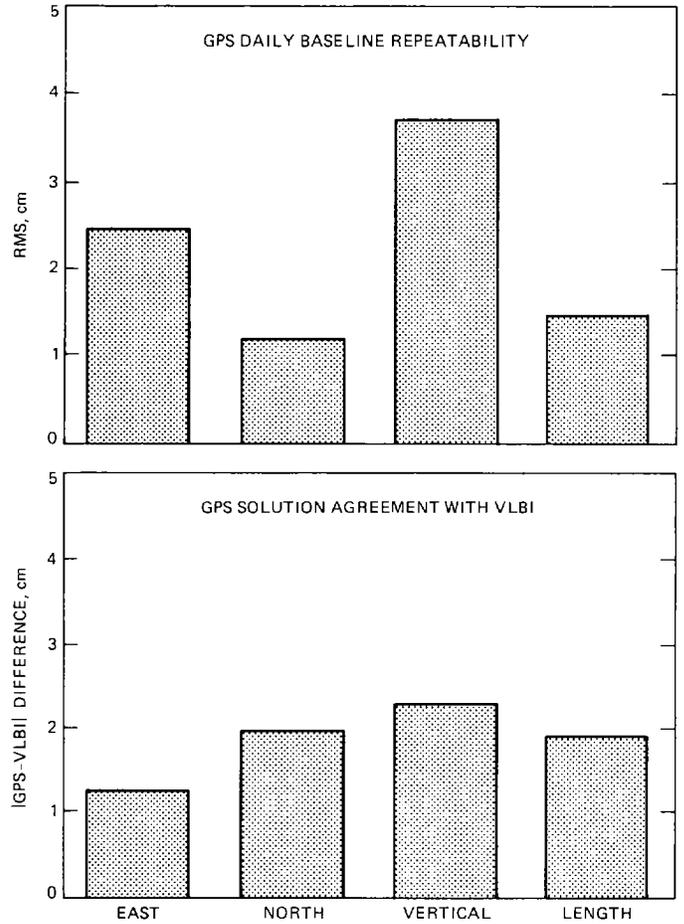

Fig. 10. Daily GPS baseline repeatability and agreement with VLBI for the Richmond-Haystack 2046-km baseline determined with a multiday orbit fit from Nov. 13-24, 1985.
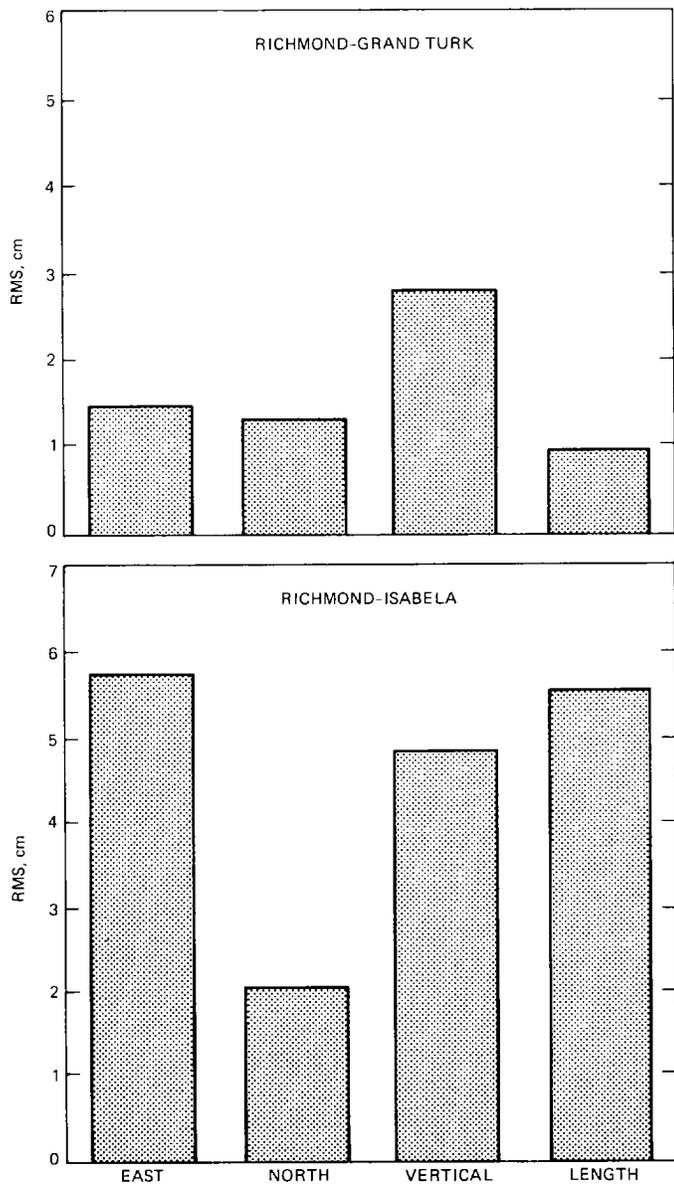
Fig. 11. Daily GPS baseline repeatability for two baselines (1049 and 1582 km) to the Caribbean region determined with multiday arc orbits from the June 1986 experiment.